



Theoretical and numerical approaches for Vlasov–Maxwell equations

Charge-conserving grid based methods for the Vlasov–Maxwell equations



Nicolas Crouseilles^a, Pierre Navaro^b, Éric Sonnendrücker^{c,d,*}

^a Inria Rennes Bretagne Atlantique, IPSO Project, France

^b IRMA – CNRS & Université de Strasbourg, France

^c Max-Planck Institute for Plasma Physics, Boltzmannstr. 2, 85748 Garching, Germany

^d Mathematics Center, TU Munich, Boltzmannstr. 3, 85747 Garching, Germany

ARTICLE INFO

Article history:

Received 11 April 2014

Accepted 10 June 2014

Available online 7 August 2014

Keywords:

Maxwell–Vlasov system

Discrete continuity equation

Finite volume method

Spectral method

Semi-Lagrangian method

ABSTRACT

In this article, we introduce numerical schemes for the Vlasov–Maxwell equations relying on different kinds of grid-based Vlasov solvers, as opposite to PIC schemes, which enforce a discrete continuity equation. The idea underlying these schemes relies on a time-splitting scheme between configuration space and velocity space for the Vlasov equation and on the computation of the discrete current in a form that is compatible with the discrete Maxwell solver.

© 2014 Académie des sciences. Published by Elsevier Masson SAS. All rights reserved.

1. Introduction

We consider the motion of particles in their self-consistent electromagnetic field, which can be described by the Vlasov–Maxwell equations. In this work, we restrict ourselves to the two-dimensional non-relativistic model, which involves four phase space dimensions, namely x, y, v_x, v_y , but the ideas developed here can be extended in a straightforward manner to the 3D relativistic model. In our case, the unknown quantities are the particle distribution function $f(t, \mathbf{x}, \mathbf{v})$, the electric field $\mathbf{E}(t, \mathbf{x}) = (E_x, E_y, 0)$, and the magnetic field $\mathbf{B}(t, \mathbf{x}) = (0, 0, B_z)$, where $\mathbf{x} = (x, y)$ and $\mathbf{v} = (v_x, v_y)$. Then the Vlasov equation reads

$$\frac{\partial f}{\partial t} + \mathbf{v} \cdot \nabla_x f + (\mathbf{E}(t, \mathbf{x}) + \mathbf{v} \times \mathbf{B}(t, \mathbf{x})) \cdot \nabla_v f = 0 \quad (1)$$

where ∇_x denotes the gradient in configuration space and ∇_v denotes the gradient in velocity space. The initial condition $f(0, \mathbf{x}, \mathbf{v}) = f_0(\mathbf{x}, \mathbf{v})$ is given. The self-consistent electromagnetic field $(\mathbf{E}(t, \mathbf{x}), \mathbf{B}(t, \mathbf{x}))$ is computed thanks to Maxwell's equations:

$$\frac{\partial \mathbf{E}}{\partial t} - \nabla \times \mathbf{B} = -\mathbf{J} \quad (2)$$

$$\frac{\partial \mathbf{B}}{\partial t} + \nabla \times \mathbf{E} = 0 \quad (3)$$

* Corresponding author.

$$\nabla \cdot \mathbf{E} = \rho \tag{4}$$

$$\nabla \cdot \mathbf{B} = 0 \tag{5}$$

The source of Maxwell’s equations, namely the charge density ρ and the current density $\mathbf{J} = (J_x, J_y)$, are computed from the particle distribution f and the uniform neutralizing Maxwellian background particles defined by their density $n_b(\mathbf{x}) = \int f_0(\mathbf{x}, \mathbf{v}) \, d\mathbf{v}$ thanks to

$$\rho(t, \mathbf{x}) = \int_{\mathbb{R}^2} (f(t, \mathbf{x}, \mathbf{v}) \, d\mathbf{v} - n_b(\mathbf{x})), \quad \mathbf{J}(t, \mathbf{x}) = \int_{\mathbb{R}^2} f(t, \mathbf{x}, \mathbf{v}) \mathbf{v} \, d\mathbf{v} \tag{6}$$

Note that integrating the Vlasov equation (1) with respect to the velocity variable \mathbf{v} yields

$$\frac{\partial \rho}{\partial t} + \nabla \cdot \mathbf{J} = 0 \tag{7}$$

which is called the continuity equation and expresses the local conservation of charge. In the continuous setting, provided this continuity equation is satisfied and Gauss’ law (4) is satisfied at time $t = 0$, if the electric and magnetic fields are computed using only Ampère’s law (2) and Faraday’s law (3); Gauss’ law is satisfied for all time. In general, numerical Vlasov–Maxwell solvers being PIC, Eulerian or semi-Lagrangian do not verify this and a correction scheme is generally used to enforce Gauss’ law at each time step or from time to time, see [1].

The aim of this paper is to propose a general procedure, valid for Vlasov solvers on a Cartesian grid based on a splitting method between configuration and velocity space, which enables us to establish a discrete continuity equation verified by the discrete charge and current densities computed from the Vlasov solver, compatible with the Maxwell solver, so that only Ampère’s and Faraday’s laws will need to be advanced by our Maxwell solver, Gauss’ law being a consequence of those.

The outline of the paper is as follows. First we will derive the discrete continuity equations associated with the Yee Maxwell solver and with a spectral solver, then we will introduce an algorithm for computing the discrete charge and current densities compatible with these discrete continuity equations for a conservative semi-Lagrangian algorithm and a spectral algorithm. Finally, after presenting the coupling algorithm, we will validate our method on some relevant test cases.

2. Discrete continuity equations

A discrete continuity equation is necessarily linked to the Maxwell solver, as the discrete curl and divergence operators need to be compatible. To this aim a first requirement of the Maxwell solver is that the discrete divergence of the discrete curl vanishes. In this case, a discrete continuity equation specific for each solver can be derived such that if this discrete continuity equation is satisfied and the Gauss law is satisfied at time step $t^n = n\Delta t$, it will also be satisfied at time step t^{n+1} .

The formulation of the discrete continuity equation for the Yee scheme, as well as for finite-volume schemes for the Maxwell system on unstructured grids with the leap-frog and other time stepping schemes, has already been obtained by Bouchut [2].

We shall recall here the discrete continuity equation for the classical Yee solver and also introduce it for a spectral solver associated with a leap-frog method in time.

2.1. For the Yee–Maxwell solver

Let us first consider the classical Yee solver on a staggered mesh. Fig. 1 displays the positions of the different components of the fields on a staggered Cartesian grid in the Yee scheme.

The Yee scheme reads

$$\frac{E_{x_{i+1/2,j}}^{n+1} - E_{x_{i+1/2,j}}^n}{\Delta t} = c^2 \frac{B_{z_{i+1/2,j+1/2}}^n - B_{z_{i+1/2,j-1/2}}^n}{\Delta y} - \frac{1}{\epsilon_0} J_{x_{i+1/2,j}}^{n+1/2} \tag{8}$$

$$\frac{E_{y_{i,j+1/2}}^{n+1} - E_{y_{i,j+1/2}}^n}{\Delta t} = -c^2 \frac{B_{z_{i+1/2,j+1/2}}^n - B_{z_{i-1/2,j+1/2}}^n}{\Delta x} - \frac{1}{\epsilon_0} J_{y_{i,j+1/2}}^{n+1/2} \tag{9}$$

$$\frac{B_{z_{i+1/2,j+1/2}}^{n+1} - B_{z_{i+1/2,j+1/2}}^n}{\Delta t} = \frac{E_{x_{i+1/2,j+1}}^n - E_{x_{i+1/2,j}}^n}{\Delta y} - \frac{E_{y_{i+1,j+1/2}}^n - E_{y_{i,j+1/2}}^n}{\Delta x} \tag{10}$$

The associated discrete Gauss’ law at time t^n will then read

$$\frac{E_{x_{i+1/2,j}}^n - E_{x_{i-1/2,j}}^n}{\Delta x} + \frac{E_{y_{i,j+1/2}}^n - E_{y_{i,j-1/2}}^n}{\Delta y} = \frac{1}{\epsilon_0} \rho_{i,j}^n \tag{11}$$

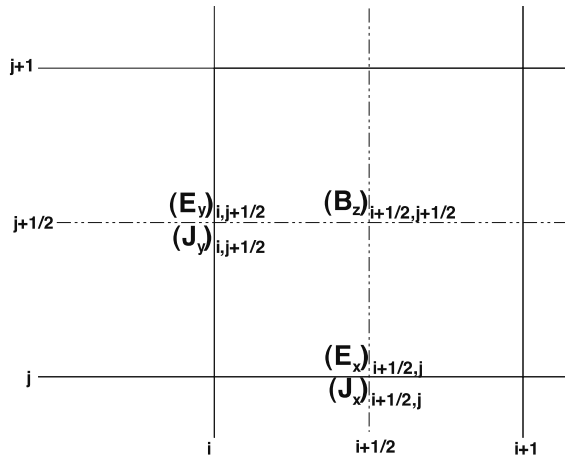


Fig. 1. Positions of the different components of the fields in the Yee scheme.

Now, taking the discrete divergence of Ampère’s law (8)–(9) yields

$$\frac{1}{\Delta t} \left(\frac{E_{x_{i+1/2,j}}^{n+1} - E_{x_{i-1/2,j}}^{n+1}}{\Delta x} + \frac{E_{y_{i,j+1/2}}^{n+1} - E_{y_{i,j-1/2}}^{n+1}}{\Delta y} - \frac{E_{x_{i+1/2,j}}^n - E_{x_{i-1/2,j}}^n}{\Delta x} - \frac{E_{y_{i,j+1/2}}^n - E_{y_{i,j-1/2}}^n}{\Delta y} \right) = -\frac{1}{\epsilon_0} \left(\frac{J_{x_{i+1/2,j}}^n - J_{x_{i-1/2,j}}^n}{\Delta x} + \frac{J_{y_{i,j+1/2}}^{n+1/2} - J_{y_{i,j-1/2}}^{n+1/2}}{\Delta y} \right) \tag{12}$$

Let us now introduce, at time step t^n , the following discrete continuity

$$\frac{\rho_{i,j}^{n+1} - \rho_{i,j}^n}{\Delta t} + \frac{J_{x_{i+1/2,j}}^n - J_{x_{i-1/2,j}}^{n+1/2}}{\Delta x} + \frac{J_{y_{i,j+1/2}}^n - J_{y_{i,j-1/2}}^{n+1/2}}{\Delta y} = 0 \tag{13}$$

If this is satisfied, it follows from (12) that

$$\frac{1}{\Delta t} \left(\frac{E_{x_{i+1/2,j}}^{n+1} - E_{x_{i-1/2,j}}^{n+1}}{\Delta x} + \frac{E_{y_{i,j+1/2}}^{n+1} - E_{y_{i,j-1/2}}^{n+1}}{\Delta y} - \frac{E_{x_{i+1/2,j}}^n - E_{x_{i-1/2,j}}^n}{\Delta x} - \frac{E_{y_{i,j+1/2}}^n - E_{y_{i,j-1/2}}^n}{\Delta y} \right) = \frac{1}{\epsilon_0} \left(\frac{\rho_{i,j}^{n+1} - \rho_{i,j}^n}{\Delta t} \right)$$

So, if the discrete Gauss law (11) is satisfied at time t^n , it follows that

$$\frac{E_{x_{i+1/2,j}}^{n+1} - E_{x_{i-1/2,j}}^{n+1}}{\Delta x} + \frac{E_{y_{i,j+1/2}}^{n+1} - E_{y_{i,j-1/2}}^{n+1}}{\Delta y} = \frac{1}{\epsilon_0} \rho_{i,j}^{n+1}$$

which is the discrete Gauss law at time t^{n+1} .

2.2. For a spectral Maxwell solver

We consider periodic boundary conditions in x and y so that a discrete Fourier transform is adapted to the spatial discretization of the Vlasov and Maxwell equations. We denote by E_{x,k_x,k_y}^n the spatial discrete Fourier transform of $E_x(t^n)$ —similar notations are used for E_y, B_z, ρ, J_x and J_y —with $t^n = n\Delta t, n \in \mathbb{N}, \Delta t > 0$. Then the Fourier transform in (x, y) of the Faraday and Ampère equations together with a leap-frog scheme in time lead to the following Maxwell solver:

$$\frac{E_{x,k_x,k_y}^{n+1} - E_{x,k_x,k_y}^n}{\Delta t} = ik_y B_{z,k_x,k_y}^n - J_{x,k_x,k_y}^{n+1/2} \tag{14}$$

$$\frac{E_{y,k_x,k_y}^{n+1} - E_{y,k_x,k_y}^n}{\Delta t} = -ik_x B_{z,k_x,k_y}^n - J_{y,k_x,k_y}^{n+1/2} \tag{15}$$

$$\frac{B_{z,k_x,k_y}^{n+1/2} - B_{z,k_x,k_y}^{n-1/2}}{\Delta t} = ik_y E_{x,k_x,k_y}^n - ik_x E_{y,k_x,k_y}^n \tag{16}$$

The discrete spectral Gauss' law at time t^n writes

$$ik_x E_{x,k_x,k_y}^n + ik_y E_{y,k_x,k_y}^n = \rho_{k_x,k_y}^n \tag{17}$$

Taking the discrete Ampère law in the spectral case amounts to summing (14) multiplied by ik_x and (15) multiplied by ik_y . This leads to

$$\frac{1}{\Delta t} (ik_x E_{x,k_x,k_y}^{n+1} + ik_y E_{y,k_x,k_y}^{n+1} - ik_x E_{x,k_x,k_y}^n - ik_y E_{y,k_x,k_y}^n) = -(ik_x J_{x,k_x,k_y}^n + ik_y J_{y,k_x,k_y}^n)$$

Notice that here also, like in the Yee scheme, the discrete curl of B_z vanishes in the last equation, which is a necessary property for our Maxwell solvers if we want a discrete continuity equation. Since the Gauss law (17) is satisfied at time t^n , we then have:

$$ik_x E_{x,k_x,k_y}^{n+1} + ik_y E_{y,k_x,k_y}^{n+1} = \rho_{k_x,k_y}^n - \Delta t (ik_x J_{x,k_x,k_y}^n + ik_y J_{y,k_x,k_y}^n) \tag{18}$$

The discrete version of the continuity equation (7) reads here

$$\rho_{k_x,k_y}^{n+1} = \rho_{k_x,k_y}^n - \Delta t (ik_x J_{x,k_x,k_y}^{n+1/2} + ik_y J_{y,k_x,k_y}^{n+1/2}) \tag{19}$$

If this is ensured, it follows from (18) that

$$ik_x E_{x,k_x,k_y}^{n+1} + ik_y E_{y,k_x,k_y}^{n+1} = \rho_{k_x,k_y}^{n+1}$$

which is the Gauss law, is satisfied at time t^{n+1} .

3. Computation of the discrete charge and current density from the Vlasov solver compatible with the discrete continuity equation

Having identified the discrete continuity equation for the Maxwell solver that we want to use, the next task is to find a way to compute the discrete charge and current densities from the Vlasov equation so that they satisfy this discrete continuity equation.

For Particle-In-Cell (PIC) Vlasov solvers associated with the Yee–Maxwell solver, there is a well-known procedure for doing that, introduced by Villasenor and Buneman [3], generalised to higher-order deposition schemes in [4]. Other options are also possible, like those introduced by Esirkepov [5] or Umeda [6].

In the case of grid-based Vlasov solvers, Sircombe and Arber [7] showed that this could be enforced for a split-Eulerian Vlasov solver using the PPM method of Colella and Woodward [8] by computing \mathbf{J} from the fluxes needed by the algorithm in the configuration space advections. Let us now show that this idea can be applied for general finite-volume schemes, including, as we will see, conservative semi-Lagrangian schemes.

A splitting of the Vlasov equation between configuration space and velocity space advection will lead us to solve alternatively

$$\frac{\partial f}{\partial t} + \mathbf{v} \cdot \nabla_x f = 0 \tag{20}$$

and

$$\frac{\partial f}{\partial t} + \frac{q}{m} (\mathbf{E}(t, \mathbf{x}) + \mathbf{v} \times \mathbf{B}(t, \mathbf{x})) \cdot \nabla_v f = 0 \tag{21}$$

The second equation does not modify ρ as can be seen when integrating with respect to momentum. Hence it should not provide any direct contribution to \mathbf{J} either for the discrete continuity equation to be satisfied. We shall only require that the discrete solver exactly conserves ρ at all grid points, which is the case for all conservative solvers. So assuming that a conservative solver is used for the velocity space advection, our problem is now to design a configuration space advection compatible with the discrete continuity equation given by the Maxwell solver.

We first notice that the advection in configuration space (20) is for each given \mathbf{v} a constant-coefficient advection. Note that this would be true also in the relativistic case for each given \mathbf{p} .

We shall further split the configuration space advection for fixed \mathbf{v} into two 1D advections, which is simpler and less costly. Note that this does not introduce any additional splitting error, as constant-coefficient advections commute.

Finally, we only need to consider constant-coefficient 1D advections of the form

$$\frac{\partial f}{\partial t} + a \frac{\partial f}{\partial x} = 0 \tag{22}$$

with a being v_x or v_y at a given velocity grid point.

We shall provide compatible schemes in the case of the finite-volume and spectral methods we consider.

3.1. Finite-volume schemes

Let us define uniformly spaced-control cells $[x_{i-1/2}, x_{i+1/2}]$ with $x_{i+1/2} - x_{i-1/2} = \Delta x$. The unknown in a finite-volume scheme will be the average value on a control cell that we shall denote by

$$f_i = \frac{1}{\Delta x} \int_{x_{i-1/2}}^{x_{i+1/2}} f(x) dx$$

Integrating (22) on a control cell and between time t^n and t^{n+1} yields:

$$f_i^{n+1} = f_i^n - \frac{a}{\Delta x} \int_{t^n}^{t^{n+1}} (f(t, x_{i+1/2}) - f(t, x_{i-1/2})) dt$$

Let us denote by $f_{i+1/2}^{n+1/2}$ a numerical approximation of $\frac{1}{\Delta t} \int_{t^n}^{t^{n+1}} f(t, x_{i+1/2}) dt$. Then our finite-volume scheme becomes:

$$f_i^{n+1} = f_i^n - \frac{a\Delta t}{\Delta x} (f_{i+1/2}^{n+1/2} - f_{i-1/2}^{n+1/2}) \quad (23)$$

Note that the actual computation of $f_{i+1/2}^{n+1/2}$ makes up the specific finite-volume scheme, this could be done with an upwind scheme or the PPM scheme or other. For our purposes, it will be sufficient to consider this generic form of the finite-volume scheme.

Let us now come back to our split Vlasov solver, for which a finite-volume scheme of the form (23) will be used in the x and y advection steps and any conservative scheme in the \mathbf{v} advection step. We discretize the distribution function on a 4D grid with uniform steps in each direction, denoting by i the x index, j the y index, k the v_x index and l the v_y index. Starting from $f_{i,j,k,l}^n$ at time step t^n , the algorithm reads,

$$\begin{aligned} f_{i,j,k,l}^{n,1} &= f_{i,j,k,l}^n - \frac{v_{x,k,l}\Delta t}{2\Delta x} (f_{i+1/2,j,k,l}^{n,1/2} - f_{i-1/2,j,k,l}^{n,1/2}) \\ f_{i,j,k,l}^{n,2} &= f_{i,j,k,l}^{n,1} - \frac{v_{y,k,l}\Delta t}{2\Delta y} (f_{i,j+1/2,k,l}^{n,3/2} - f_{i,j-1/2,k,l}^{n,3/2}) \\ f_{i,j,k,l}^{n,3} &\leftarrow f_{i,j,k,l}^{n,2} \quad \text{using a conservative advection in } \mathbf{v} \text{ space} \\ f_{i,j,k,l}^{n,4} &= f_{i,j,k,l}^{n,3} - \frac{v_{y,k,l}\Delta t}{2\Delta y} (f_{i,j+1/2,k,l}^{n,7/2} - f_{i,j-1/2,k,l}^{n,7/2}) \\ f_{i,j,k,l}^{n+1} &= f_{i,j,k,l}^{n,4} - \frac{v_{x,k,l}\Delta t}{2\Delta x} (f_{i+1/2,j,k,l}^{n,9/2} - f_{i-1/2,j,k,l}^{n,9/2}) \end{aligned}$$

Now, the discrete charge density is linked to the discrete distribution function by

$$\rho_{i,j}^n = q\Delta v_x\Delta v_y \sum_k \sum_l f_{i,j,k,l}^n$$

So, using the previous algorithm we can relate $\rho_{i,j}^{n+1}$ to $\rho_{i,j}^n$ by summing the different lines with respect to k, l . Then, we get

$$\begin{aligned} \frac{1}{q\Delta v_x\Delta v_y} \rho_{i,j}^{n+1} &= \sum_{k,l} f_{i,j,k,l}^{n+1} \\ &= \sum_{k,l} f_{i,j,k,l}^{n,4} - \frac{\Delta t}{2\Delta x} \sum_{k,l} v_{x,k,l} (f_{i+1/2,j,k,l}^{n,9/2} - f_{i-1/2,j,k,l}^{n,9/2}) \\ &= \sum_{k,l} f_{i,j,k,l}^{n,3} - \frac{\Delta t}{2\Delta y} \sum_{k,l} v_{y,k,l} (f_{i,j+1/2,k,l}^{n,7/2} - f_{i,j-1/2,k,l}^{n,7/2}) \\ &\quad - \frac{\Delta t}{2\Delta x} \sum_{k,l} v_{x,k,l} (f_{i+1/2,j,k,l}^{n,9/2} - f_{i-1/2,j,k,l}^{n,9/2}) \end{aligned}$$

Then the conservativity of the advection in \mathbf{v} space yields $\sum_{k,l} f_{i,j,k,l}^{n,3} = \sum_{k,l} f_{i,j,k,l}^{n,2}$. Thus, proceeding in the same manner with the first two steps of the algorithm, we finally get:

$$\frac{1}{q\Delta v_x\Delta v_y}\rho_{i,j}^{n+1} = \sum_{k,l} f_{i,j,k,l}^n - \frac{\Delta t}{2\Delta y} \sum_{k,l} (v_{y,k,l}(f_{i,j+1/2,k,l}^{n,7/2} + f_{i,j+1/2,k,l}^{n,3/2} - f_{i,j-1/2,k,l}^{n,7/2} - f_{i,j-1/2,k,l}^{n,3/2}) - v_{x,k,l}(f_{i+1/2,j,k,l}^{n,9/2} + f_{i+1/2,j,k,l}^{n,1/2} - f_{i-1/2,j,k,l}^{n,9/2} - f_{i-1/2,j,k,l}^{n,1/2})) \tag{24}$$

Let us now denote:

$$J_{x_{i+1/2,j}}^{n+1/2} = q\Delta v_x\Delta v_y \sum_{k,l} v_{x,k,l} \cdot \frac{1}{2}(f_{i+1/2,j,k,l}^{n,9/2} + f_{i+1/2,j,k,l}^{n,1/2}) \tag{25}$$

$$J_{y_{i,j+1/2}}^{n+1/2} = q\Delta v_x\Delta v_y \sum_{k,l} v_{y,k,l} \cdot \frac{1}{2}(f_{i,j+1/2,k,l}^{n,7/2} + f_{i,j+1/2,k,l}^{n,3/2}) \tag{26}$$

then (24) becomes

$$\frac{\rho_{i,j}^{n+1} - \rho_{i,j}^n}{\Delta t} + \frac{J_{x_{i+1/2,j}}^{n+1/2} - J_{x_{i-1/2,j}}^{n+1/2}}{\Delta x} + \frac{J_{y_{i,j+1/2}}^{n+1/2} - J_{y_{i,j-1/2}}^{n+1/2}}{\Delta y} = 0$$

which is exactly the discrete continuity equation (13) needed by the Yee scheme. Hence expressions (25)–(26) provide an expression of the discrete current density **J** consistent with a finite-volume Vlasov solver and that satisfies a discrete continuity equation.

3.2. Finite-volume form of a semi-Lagrangian scheme

We have obtained in the previous section an explicit expression for the discrete current that satisfies a discrete continuity equation for any split Vlasov solver for which the *x* and *y* advection parts can be cast in the generic finite-volume framework (23). We are now going to cast a conservative semi-Lagrangian scheme [9] for constant-coefficient advection into this finite-volume formalism. This will then enable us to construct charge conserving algorithms for a large class of split semi-Lagrangian schemes.

In both finite-volume and conservative semi-Lagrangian schemes, the first step is to reconstruct a piecewise polynomial function on each cell. We shall call f^R this reconstructed piecewise polynomial function. The reconstruction scheme does not matter for our purpose; it could be PPM, splines or something else, with limiters or not. The only property we shall need is that it is linked to the computed cell averages $f_j = \frac{1}{\Delta x} \int_{x_{j-1/2}}^{x_{j+1/2}} f(x) dx$, by

$$f_j = \frac{1}{\Delta x} \int_{x_{j-1/2}}^{x_{j+1/2}} f^R(x) dx$$

We shall also assume that the CFL condition $\frac{a\Delta t}{\Delta x} \leq 1$ is verified.

In a finite-volume scheme for the 1D advection equation (22), we then compute

$$f_{i+1/2}^{n+1/2} = \frac{1}{\Delta t} \int_{t^n}^{t^{n+1}} f(t, x_{i+1/2}) dt = \frac{1}{\Delta t} \int_{t^n}^{t^{n+1}} f^R(x_{i+1/2} - a(t - t^n)) dt$$

and by the change of variables $x = x_{i+1/2} - a(t - t^n)$

$$f_{i+1/2}^{n+1/2} = \frac{1}{a\Delta t} \int_{x_{i+1/2}-a\Delta t}^{x_{i+1/2}} f^R(x) dx$$

Then using the formulation (23), we get the finite-volume scheme

$$f_i^{n+1} = f_i^n - \frac{1}{\Delta x} \left(\int_{x_{i+1/2}-a\Delta t}^{x_{i+1/2}} f^R(x) dx - \int_{x_{i-1/2}-a\Delta t}^{x_{i-1/2}} f^R(x) dx \right) \tag{27}$$

On the other hand, for a conservative semi-Lagrangian scheme, the distribution function is updated using the relation

$$f_i^{n+1} = \frac{1}{\Delta x} \int_{X(x_{j-1/2})}^{X(x_{j+1/2})} f^R(x) dx$$

where $X(x_{j+1/2})$ is the origin of the characteristic ending at $x_{j+1/2}$, that is in our case of constant advection at velocity a , $X(x_{j+1/2}) = x_{j+1/2} - a\Delta t$. Hence

$$\begin{aligned} f_i^{n+1} &= \frac{1}{\Delta x} \int_{x_{j-1/2}-a\Delta t}^{x_{j+1/2}-a\Delta t} f^R(x) dx \\ &= \frac{1}{\Delta x} \left(\int_{x_{j-1/2}-a\Delta t}^{x_{j-1/2}} f^R(x) dx + \int_{x_{j-1/2}}^{x_{j+1/2}} f^R(x) dx - \int_{x_{j+1/2}-a\Delta t}^{x_{j+1/2}} f^R(x) dx \right) \\ &= f_i^n + \frac{1}{\Delta x} \left(\int_{x_{j-1/2}-a\Delta t}^{x_{j-1/2}} f^R(x) dx - \int_{x_{j+1/2}-a\Delta t}^{x_{j+1/2}} f^R(x) dx \right) \end{aligned}$$

which is the same expression as (27), so that both formalisms yield the same numerical scheme. Moreover, the finite volume flux $f_{i+1/2}^{n+1/2}$ can be expressed for a semi-Lagrangian scheme with respect to the reconstructed function f^R by

$$f_{i+1/2}^{n+1/2} = \int_{x_{j+1/2}-a\Delta t}^{x_{j+1/2}} f^R(x) dx$$

In particular, if the reconstruction is performed using a primitive F^R of f^R , we have:

$$f_{i+1/2}^{n+1/2} = F^R(x_{j+1/2}) - F^R(x_{j+1/2} - a\Delta t)$$

It now remains to provide the fluxes for both half advections in x and y . For the half-advections in x , we have, on the one hand, integrating on $[t^n, t^{n+1}] \times [x_{i-1/2}, x_{i+1/2}]$:

$$\begin{aligned} f_i^{n,1} &= f_i^n - \frac{v_x \Delta t}{2\Delta x} \int_{t^n}^{t^{n+1}} [f(t, x_{i+1/2}) - f(t, x_{i-1/2})] dt \\ &= f_i^n - \frac{v_x \Delta t}{2\Delta x} [f_{i+1/2}^{n,1/2} - f_{i-1/2}^{n,1/2}] \end{aligned} \quad (28)$$

with $f_{i+1/2}^{n,1/2} = \int_{t^n}^{t^{n+1}} f(t, x_{i+1/2}) dt$. On the other hand,

$$\begin{aligned} f_i^{n,1} &:= \frac{1}{\Delta x} \int_{x_{i-1/2}}^{x_{i+1/2}} f^{n,1}(x) dx = \frac{1}{\Delta x} \int_{x_{i-1/2}-v_x \Delta t/2}^{x_{i+1/2}-v_x \Delta t/2} f^n(x) dx \\ &= f_i^n - \frac{1}{\Delta x} [\phi_{i+1/2}^{n,1/2} - \phi_{i-1/2}^{n,1/2}] \end{aligned} \quad (29)$$

with $\phi_{i+1/2}^{n,1} = \int_{x_{i+1/2}-v_x \Delta t/2}^{x_{i+1/2}} f^n(x) dx$. Hence, identifying the fluxes in (28) and (29), we have

$$f_{i+1/2}^{n,1/2} = \begin{cases} \phi_{i+1/2}^{n,1/2}/(v_x \Delta t/2) & \text{if } v_x \neq 0 \\ 0 & \text{if } v_x = 0 \end{cases}$$

In the same way for $f_{i+1/2}^{n,9/2}$, we have

$$f_{i+1/2}^{n,9/2} = \begin{cases} \phi_{i+1/2}^{n,9/2}/(v_x \Delta t/2) & \text{if } v_x \neq 0 \\ 0 & \text{if } v_x = 0 \end{cases}$$

Then $\phi_{i+1/2}^{n,1/2} = F(x_{i+1/2}) - F(x_{i+1/2} - v_x \Delta t/2)$ with F the primitive of f^n , $\phi_{i+1/2}^{n,9/2} = F(x_{i+1/2}) - F(x_{i+1/2} - v_x \Delta t/2)$ with F the primitive of $f^{n,4}$.

For the half-advections in y , we proceed in the same way integrating on $[t^n, t^{n+1}] \times [y_{j-1/2}, y_{j+1/2}]$ in order to obtain the finite volume formulation (as (28)) and identifying with the conservative semi-Lagrangian formulation (as (29)), we have:

$$f_{j+1/2}^{n,3/2} = \begin{cases} \phi_{j+1/2}^{n,3/2}/(v_y \Delta t/2) & \text{if } v_y \neq 0 \\ 0 & \text{if } v_y = 0 \end{cases}$$

and

$$f_{j+1/2}^{n,7/2} = \begin{cases} \phi_{j+1/2}^{n,7/2}/(v_y \Delta t/2) & \text{if } v_y \neq 0 \\ 0 & \text{if } v_y = 0 \end{cases}$$

Then $\phi_{j+1/2}^{n,3/2} = F(y_{j+1/2}) - F(y_{j+1/2} - v_y \Delta t/2)$ with F the primitive of $f^{n,1}$, $\phi_{j+1/2}^{n,7/2} = F(y_{j+1/2}) - F(y_{j+1/2} - v_y \Delta t/2)$ with F the primitive of $f^{n,3}$.

3.3. Spectral scheme

Denoting by $f^n(k_x, k_y, v_x, v_y)$ the Fourier transform in space of $f(t^n)$, the 1D advections in configuration space become for the spectral scheme

$$\frac{\partial f}{\partial t} + ik_x v_x f = 0 \tag{30}$$

for which the exact solution on a time step reads $f(t + \Delta t) = f(t) \exp(-ik_x v_x \Delta t)$, and the same for the advection in y .

So, using a spectral scheme in space coupled with a Strang splitting, we get the following algorithm

$$\begin{aligned} f_{k_x, k_y, k, l}^{n,1} &= f_{k_x, k_y, k, l}^n \exp(-ik_x v_x \Delta t/2) \\ f_{k_x, k_y, k, l}^{n,2} &= f_{k_x, k_y, k, l}^{n,1} \exp(-ik_y v_y \Delta t/2) \\ f_{k_x, k_y, k, l}^{n,3} &\leftarrow f_{k_x, k_y, k, l}^{n,2} \quad \text{using a conservative advection in the } \mathbf{v} \text{ space} \\ f_{k_x, k_y, k, l}^{n,4} &= f_{k_x, k_y, k, l}^{n,3} \exp(-ik_y v_y \Delta t/2) \\ f_{k_x, k_y, k, l}^{n+1} &= f_{k_x, k_y, k, l}^{n,4} \exp(-ik_x v_x \Delta t/2) \end{aligned}$$

As we did for the finite-volume schemes, we need to extract the current from the space advections in a way that is compatible with the discrete continuity equation (19) for the Maxwell solver that we want to couple to. To this aim, we need to make a transport structure appear. Introducing $f_{k_x, k_y, k, l}^{n,1/2}$

$$f_{k_x, k_y, k, l}^{n,1/2} = \begin{cases} f_{k_x, k_y, k, l}^n [1 - \exp(-ik_x v_x \Delta t/2)] / (ik_x \Delta t/2) & \text{if } k_x \neq 0 \\ 0 & \text{if } k_x = 0 \end{cases} \tag{31}$$

the first advection in x writes

$$f_{k_x, k_y, k, l}^{n,1} = f_{k_x, k_y, k, l}^n - ik_x \frac{\Delta t}{2} f_{k_x, k_y, k, l}^{n,1/2}$$

A current J_x can be now clearly identified:

$$J_{x, k_x, k_y} = \begin{cases} \sum_{k, l} f_{k_x, k_y, k, l}^{n,1/2} \Delta v_x \Delta v_y & \text{if } k_x \neq 0 \\ 0 & \text{if } k_x = 0 \end{cases}$$

Using the same notations, one has for the last x -advection (the indices k_x, k_y, k, l are omitted)

$$f^{n+1} = f^{n,4} - ik_x \frac{\Delta t}{2} f^{n,9/2}$$

where $f^{n,9/2}$ is deduced from (31) by replacing f^n by $f^{n,4}$. Similarly, for the y -advections, one has:

$$f^{n,2} = f^{n,1} - ik_y \frac{\Delta t}{2} f^{n,3/2}$$

and

$$f^{n,4} = f^{n,3} - ik_y \frac{\Delta t}{2} f^{n,7/2}$$

where $f^{n,3/2}$ and $f^{n,7/2}$ are given by ($d = 0$ or 2)

$$f_{k_x, k_y, k, l}^{n, d+3/2} = \begin{cases} f_{k_x, k_y, k, l}^{n, (d+1)} [1 - \exp(-ik_y v_y \Delta t/2)] / (ik_y \Delta t/2) & \text{if } k_y \neq 0 \\ 0 & \text{if } k_y = 0 \end{cases} \tag{32}$$

Now, let us add up the different contributions to the current. First, the discrete charge density is linked to the discrete distribution function by

$$\rho_{k_x, k_y}^n = \Delta v_x \Delta v_y \sum_k \sum_l f_{k_x, k_y, k, l}^n$$

So, using the previous algorithm we can relate ρ_{k_x, k_y}^{n+1} to ρ_{k_x, k_y}^n by summing the different lines with respect to k, l . Then, we get

$$\begin{aligned} \frac{1}{\Delta v_x \Delta v_y} \rho_{k_x, k_y}^{n+1} &= \sum_{k, l} f_{k_x, k_y, k, l}^{n+1} \\ &= \sum_{k, l} \left[f_{k_x, k_y, k, l}^{n, 4} - ik_x \frac{\Delta t}{2} f^{n, 9/2} \right] \\ &= \sum_{k, l} \left[f_{k_x, k_y, k, l}^{n, 3} - ik_y \frac{\Delta t}{2} f^{n, 7/2} - ik_x \frac{\Delta t}{2} f^{n, 9/2} \right] \end{aligned}$$

Then the conservativity of the advection in the \mathbf{v} space yields $\sum_{k, l} f_{k_x, k_y, k, l}^{n, 3} = \sum_{k, l} f_{k_x, k_y, k, l}^{n, 2}$. Thus, proceeding in the same manner with the first two steps of the algorithm, we finally get:

$$\begin{aligned} \frac{1}{\Delta v_x \Delta v_y} \rho_{k_x, k_y}^{n+1} &= \sum_{k, l} f_{k_x, k_y, k, l}^n - ik_y \frac{\Delta t}{2} \sum_{k, l} (f_{k_x, k_y, k, l}^{n, 7/2} + f_{k_x, k_y, k, l}^{n, 3/2}) \\ &\quad - ik_x \frac{\Delta t}{2} \sum_{k, l} (f_{k_x, k_y, k, l}^{n, 9/2} + f_{k_x, k_y, k, l}^{n, 1/2}) \end{aligned} \tag{33}$$

Let us now denote

$$J_{x, k_x, k_y}^{n+1/2} = \Delta v_x \Delta v_y \sum_{k, l} \frac{1}{2} (f_{k_x, k_y, k, l}^{n, 9/2} + f_{k_x, k_y, k, l}^{n, 1/2}), \tag{34}$$

$$J_{y, k_x, k_y}^{n+1/2} = \Delta v_x \Delta v_y \sum_{k, l} \frac{1}{2} (f_{k_x, k_y, k, l}^{n, 7/2} + f_{k_x, k_y, k, l}^{n, 3/2}) \tag{35}$$

Then (33) becomes

$$\frac{\rho_{k_x, k_y}^{n+1} - \rho_{k_x, k_y}^n}{\Delta t} + ik_x J_{x, k_x, k_y}^{n+1/2} + ik_y J_{y, k_x, k_y}^{n+1/2} = 0$$

which is exactly the discrete continuity equation (19) needed by the spectral Maxwell scheme.

Hence expressions (34)–(35) provide an expression of the discrete current density \mathbf{J} consistent with a spectral Vlasov solver and that satisfies a discrete continuity equation.

4. Coupling the Vlasov solver with the Maxwell solver

The only point that is not straightforward in the coupling of our Vlasov solvers with their corresponding Maxwell solvers is how to get the electric field $E^{n+1/2}$ needed for the velocity space advection before the full current has been computed. We use here for both our methods the strategy suggested in [7]. Ampère is advanced on $\Delta t/2$ using the predicted currents J^n computed using

$$J_{x, i+1/2, j}^n = \Delta v_x \Delta v_y \sum_{k, \ell} \frac{(v_x)k}{2} (f_{i, j, k, \ell}^n + f_{i+1, j, k, \ell}^n) \tag{36}$$

$$J_{y, i, j+1/2}^n = \Delta v_x \Delta v_y \sum_{k, \ell} \frac{(v_y)k}{2} (f_{i, j, k, \ell}^n + f_{i, j+1, k, \ell}^n) \tag{37}$$

This predicted electric field is then only used for the velocity advection and discarded. The electric field E^{n+1} will later be recomputed directly from E^n using the current $J^{n+1/2}$ verifying the discrete continuity equation.

We then get in both cases the following algorithm where the half advectons in x and y need to use the adequate formula for each solver introduced previously.

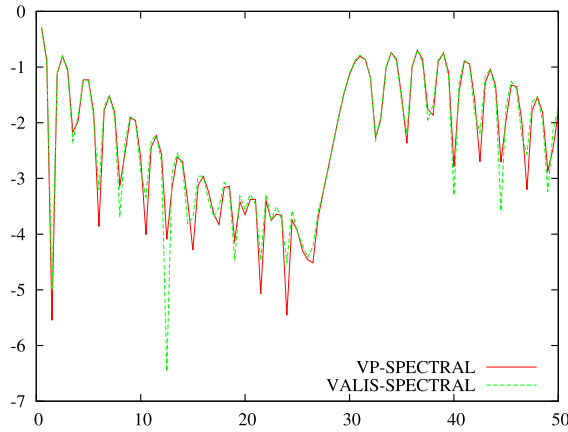


Fig. 2. (Color online.) Time history of the electric energy (log-scale): comparison of Vlasov–Poisson and VALIS (Vlasov–Maxwell equations). 16 points per spatial direction and 32 points per velocity direction. $\Delta t = 0.5$.

Algorithm Starting from $E^n = (E_x^n, E_y^n)$, $B_z^{n-1/2}$ and f^n , we compute E^{n+1} , $B_z^{n+1/2}$ and f^{n+1} as:

1. **Maxwell prediction** $\rightarrow B_z^{n+1/2}$ and $(E_x^{n+1/2}, E_y^{n+1/2})$
 - (a) advance Faraday (16) on Δt with $B_z^{n-1/2}$ and $E^n \rightarrow B_z^{n-1/2}$
 - (b) compute $J_x^n = \sum_{k,l} (v_x)_k f^n \Delta v_x \Delta v_y$ and $J_y^n = \sum_{k,l} (v_y)_l f^n \Delta v_x \Delta v_y$.
 - (c) advance Ampère (14)–(15) on $\Delta t/2$ with E^n , $B_z^{n+1/2}$ and $(J_x^n, J_y^n) \rightarrow E^{n+1/2}$
2. **half-advection in x** $\rightarrow f^{n,1}$ and $J_x^{n,1/2}$
 - (a) compute $f^{n,1/2}$ and $J_x^{n,1/2} = \sum_{k,l} (v_x)_k f^{n,1/2} \Delta v_x \Delta v_y$
 - (b) half-advection in x
3. **half-advection in y** $\rightarrow f^{n,2}$ et $J_y^{n,3/2}$
 - (a) compute $f^{n,3/2}$ and $J_y^{n,3/2} = \sum_{k,l} (v_y)_l f^{n,3/2} \Delta v_x \Delta v_y$
 - (b) half-advection in y
4. **advection in v** with $E^{n+1/2}$ and $B_z^{n+1/2} \rightarrow f^{n,3}$
5. **half-advection in y** $\rightarrow f^{n,4}$ and $J_y^{n,7/2}$
 - (a) compute $f^{n,7/2}$ and $J_y^{n,7/2} = \sum_{k,l} (v_y)_l f^{n,7/2} \Delta v_x \Delta v_y$
 - (b) half-advection in y
6. **half-advection in x** $\rightarrow f^{n+1}$ and $J_x^{n,9/2}$
 - (a) compute $f^{n,9/2}$ and $J_x^{n,9/2} = \sum_{k,l} (v_x)_k f^{n,9/2} \Delta v_x \Delta v_y$
 - (b) half-advection in x
7. **advance Maxwell** $\rightarrow E_x^{n+1}$ et E_y^{n+1}
 - (a) compute $J_x^{n+1/2} = (J_x^{n,1/2} + J_x^{n,9/2})/2$
 - (b) compute $J_y^{n+1/2} = (J_y^{n,3/2} + J_y^{n,7/2})/2$
 - (c) advance Ampère (14)–(15) on Δt with E^n , $B_z^{n+1/2}$ and $(J_x^{n+1/2}, J_y^{n+1/2}) \rightarrow E^{n+1}$.

5. Numerical results

We focus on the simple linear Landau test case. This test is quite easy to validate with Vlasov–Poisson equations, but it is however known to be difficult to validate with Vlasov–Maxwell equations. We consider the following initial condition:

$$f_0(\mathbf{x}, \mathbf{v}) = \frac{1}{2\pi} e^{-|\mathbf{v}|^2/2} (1 + 0.05 \cos(k_x x))$$

with $k_x = 0.5 = 2\pi/L_x$. The domain in space is (x, y) is $[0, 4\pi]^2$ and $\mathbf{v} \in [-6, 6]^2$.

We compare this algorithm to a standard one (PC for Predictor–Corrector). The only difference arises in step 7. of the previous algorithm: the current is computed using the following average:

$$J_x^{n+1/2} = (J_x^n + J_x^{n+1})/2, \quad J_y^{n+1/2} = (J_y^n + J_y^{n+1})/2$$

where $J_x^{n+1} = \sum_{k,l} (v_x)_k f^{n+1} \Delta v_x \Delta v_y$ and $J_y^{n+1} = \sum_{k,l} (v_y)_l f^{n+1} \Delta v_x \Delta v_y$. The reference solution will be given by a Vlasov–Poisson run where the Poisson equation is solved just before the \mathbf{v} advection.

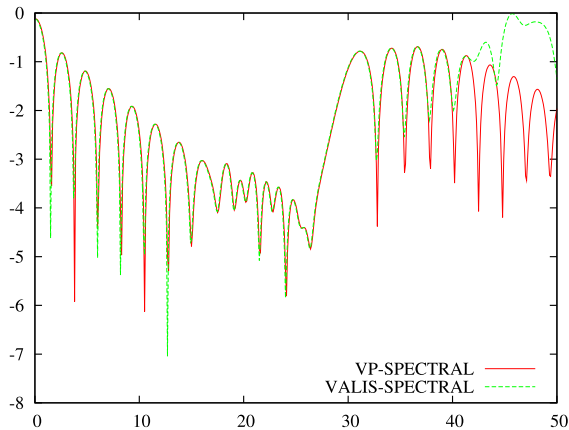


Fig. 3. (Color online.) Time history of the electric energy (log-scale): comparison of Vlasov–Poisson and VALIS (Vlasov–Maxwell equations). 32 points per direction. $\Delta t = 0.1$.

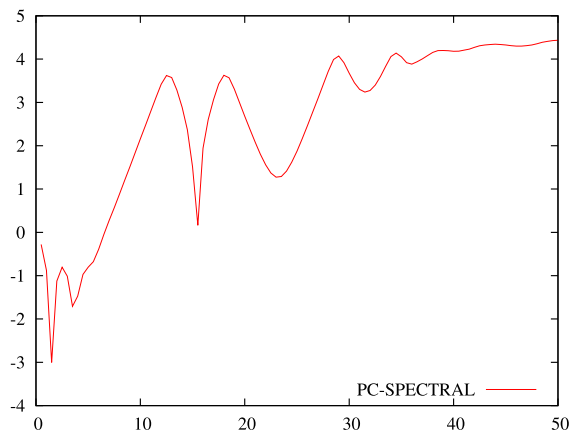


Fig. 4. (Color online.) Time history of the electric energy (log-scale): Vlasov–Maxwell equations with PC algorithm. 16 points per spatial direction and 32 points per velocity direction. $\Delta t = 0.5$.

In Figs. 2 and 3, we plot the time history of the electric energy for the reference method and the “new” method, for different numerical parameters. In Fig. 4, the results obtained with PC algorithm are displayed. Note that since the \mathbf{v} advection is performed using a 2d interpolation, the mass is not conserved exactly, which probably explains the small differences between VP and VALIS.

References

- [1] C.-D. Munz, R. Schneider, E. Sonnendrücker, U. Voss, Maxwell’s equations when the charge conservation is not satisfied, *C. R. Acad. Sci. Paris, Ser. I* 328 (5) (1999) 431–436.
- [2] F. Bouchut, On the discrete conservation of the Gauss–Poisson equation of plasma physics, *Commun. Numer. Methods Eng.* 14 (1) (1998) 23–34.
- [3] J. Villaseñor, O. Buneman, Rigorous charge conservation for local electromagnetic field solvers, *Comput. Phys. Commun.* 69 (1992) 306–316.
- [4] R. Barthelmé, C. Parzani, Numerical charge conservation in particle-in-cell codes, in: *Numerical Methods for Hyperbolic and Kinetic Problems*, in: IRMA Lect. Math. Theor. Phys., vol. 7, 2005, pp. 7–28.
- [5] Esirkepov, T. Zh, Exact charge conservation scheme for particle-in-cell simulation with an arbitrary form-factor, *Comput. Phys. Commun.* 135 (2001) 144–153.
- [6] T. Umeda, Y. Omura, T. Tominaga, H. Matsumoto, A new charge conservation method in electromagnetic particle-in-cell simulations, *Comput. Phys. Commun.* 156 (2004) 73–85.
- [7] N.J. Sircombe, T.D. Arber, VALIS: a split-conservative scheme for the relativistic 2D Vlasov–Maxwell system, *J. Comput. Phys.* 228 (2009) 4773–4788.
- [8] P. Colella, P.R. Woodward, The Piecewise Parabolic Method (PPM) for gas-dynamical simulations, *J. Comput. Phys.* 54 (1984) 174–201.
- [9] N. Crouseilles, M. Mehrenberger, E. Sonnendrücker, Conservative semi-Lagrangian schemes for the Vlasov equation, *J. Comput. Phys.* (2009).